

the blue thermoluminescence. To some extent, the more energetic 1.5-ev photons may affect also the I_b transition, and thus give also quenching of the blue band, which is in accordance with our results (see Fig. 7).

The stimulation of the green glow peak by 1.2μ seems difficult to explain by model *a*. Model *b*, however, can account for the stimulation of the green band as well as for the quenching effects. In this case irradiation by 1 ev (1.2μ) raises electrons from the blue centers up into the conduction band. Part of these electrons may then be trapped in the green traps and thus enhance the green glow as shown in Fig. 7. On irradiation with shorter wavelengths the transitions I_g enter, and cause quenching of the green peak as described above. As stated above, the more energetic photons may to some extent affect also the transition I_b and thus cause also quenching of the blue peak. The free

holes created by transition I_g seem to favor recombination with electrons in the blue centers rather than further filling up of the almost full blue traps, which again causes a reduction in the blue glow.

In some crystals no enhancement of the green glow peak was observed on irradiation with 1.2μ . Such crystals usually exhibited a very weak blue component in the glow which further supports our model.

The results seem, therefore, to be better explained by model *b*. More experimental work seems, however, to be needed before final decision about the correct model is made.

ACKNOWLEDGMENT

We are indebted to Dr. D. R. Hamilton for providing the crystals used in the present work.

Measurements of Equilibrium Vacancy Concentrations in Aluminum*

R. O. SIMMONS AND R. W. BALLUFFI
University of Illinois, Urbana, Illinois

(Received July 31, 1959)

Measurements of change in length and change in lattice parameter were made at identical temperatures on 99.995% aluminum in the temperature range 229 to 656°C. Length changes, ΔL , were measured on an unconstrained horizontal bar sample using a rigid pair of filar micrometer microscopes. X-ray lattice parameter changes, Δa , were observed using a high-angle, back-reflection, rotating-single-crystal technique. The measurements are compared to earlier work. The relative expansions $\Delta L/L$ and $\Delta a/a$ were equal within about $1:10^5$ from 229 to 415°C. At higher temperatures additional atomic sites were found to be generated: the difference between the two expansions could be represented by $3(\Delta L/L - \Delta a/a) = \exp(2.4) \exp(-0.76 \text{ ev}/kT)$. At the melting point (660°C) the equilibrium concentration of additional sites is $3(\Delta L/L - \Delta a/a) = 9.4 \times 10^{-4}$. This result is independent of the detailed

nature of the defects, for example, the lattice relaxation or degree of association. The nature of the defects is considered and it is concluded that they are predominantly lattice vacancies; it is estimated that the divacancy contribution at the melting point may well be less than about 15%, corresponding to a divacancy binding energy ≤ 0.25 ev. The observed formation energy agrees with the values obtained by quenching techniques and by interpretation of the high-temperature electrical resistivity of identical material by Simmons and Balluffi. The present work is the first direct measurement of formation entropy; the value is near that expected from theoretical considerations. The contribution of the thermally generated defects to other physical properties at high temperatures is considered briefly.

I. INTRODUCTION

THE experimental determination of the predominant atomic defects present in thermal equilibrium in metals has proven to be a difficult problem. Even though the general thermodynamic theory of point defects is well developed, experiment has not yet established the nature and concentrations of the defects in a completely satisfactory way.^{1,2} The expected equilibrium atomic fraction of the j th type

of atomic defect may be written as

$$c = g_j \exp(-G_j^f/kT) = g_j \exp(S_j^f/k) \exp(-E_j^f/kT), \quad (1)$$

where G_j^f , S_j^f and E_j^f are, respectively, the free energy of formation, the entropy of formation, both exclusive of the configurational entropy, and the energy of formation. g_j is a constant geometrical factor which depends upon the number of ways that the defect can be orientated in the lattice. Theoretical estimates of S_j^f and E_j^f for various defects indicate that vacant lattice sites are probably the predominant defects present in close-packed metals, with concentrations in the range 10^{-8} to 10^{-4} at temperatures near the melting point.³

* This work was supported by the U. S. Atomic Energy Commission.

¹ See the review papers in: *Impurities and Imperfections* (American Society for Metals, Cleveland, 1955); *Vacancies and Other Point Defects in Metals and Alloys* (The Institute of Metals, London, 1958).

² R. Feder and A. S. Nowick, *Phys. Rev.* **109**, 1959 (1958).

³ F. Seitz, in *Phase Transformation in Solids* (John Wiley & Sons, Inc., New York, 1951), p. 77.

However, these calculations are semiquantitative at best, and it is still possible that interstitial atoms may be present. Theory and experiment^{1,4-7} also suggest a binding energy between single vacancies, and presumably vacancy aggregates may also be present.

Many experimental attempts have been made to establish the quantities of Eq. (1) for the dominant point defects. In general, efforts have been made to detect the defects either directly at elevated temperatures where an appreciable concentration should exist in thermal equilibrium or at low temperatures in quenched specimens where the high-temperature concentrations are frozen in by rapid cooling. Properties such as internal friction,⁸ electrical resistivity,^{9,10} specific heat,^{10,11} linear dilatation,⁹ and release of stored energy¹² have been measured. Unfortunately, such measurements are macroscopic in nature and are not capable of identifying the type of defect. In addition, the defect concentrations cannot be obtained directly from a number of these experiments without independent information about such fundamental properties of the defects as their electrical resistivity or lattice dilatation.

There is one type of experiment, however, that appears capable of giving direct information about the nature of the predominant defects. This experiment consists of measuring differences between the fractional lattice parameter change, $\Delta a/a$, as measured by x-ray diffraction, and the linear dilatation of the specimen, $\Delta L/L$, as defects are generated in a crystal containing a constant number of atoms. Briefly, $\Delta a/a$ differs from $\Delta L/L$ since the x-rays measure only the average dilatation of the inter-atomic spacing which occurs when point imperfections are generated, whereas the macroscopic length measures both this dilatation and the dimensional changes due to the creation or destruction of substitutional atomic sites which occur when the defects are generated at sources in the crystal. The difference then gives a direct measure of the number of sites created or destroyed. For example, if vacancies are generated, new sites are created and $(\Delta L/L - \Delta a/a)$ is positive. If interstitials are generated, atomic sites are destroyed and $(\Delta L/L - \Delta a/a)$ is negative. Lattice thermal expansion does not contribute to this difference in cubic crystals because it makes equal contributions to both $\Delta L/L$ and $\Delta a/a$.

Van Duijn and Van Galen¹³ and Feder and Nowick² have made recent attempts to carry out this experiment on aluminum² and lead.^{2,13} No detectable differences between $\Delta L/L$ and $\Delta a/a$ were found for lead. However, the more recent and precise work on aluminum gave a rather questionable indication that vacancies are the predominant defect at elevated temperatures and that the fraction of thermally generated lattice sites at the melting point is 3×10^{-4} . Previous individual measurements of $\Delta L/L$ or $\Delta a/a$ by different workers using diverse methods (see Tables I and II) have not been sufficiently precise to allow an estimate of the expected small defect concentrations.

In the present work still more precise measurements of $(\Delta L/L - \Delta a/a)$ were made for high purity aluminum during heating and cooling in the temperature range between 229°C and the melting point (660°C). Aluminum was chosen because it is a cubic metal, has a relatively low melting point and evaporation rate, may be obtained in high purity form, and may be readily converted into single crystals. Every effort was made to achieve the maximum possible precision in the measurements, and simultaneous measurements of $\Delta L/L$ and $\Delta a/a$ were made on the same specimen held at constant temperature. A real difference was found between $\Delta L/L$ and $\Delta a/a$ at elevated temperatures, and the number of thermally generated lattice sites was measured with fairly satisfactory precision. The defects in thermal equilibrium were identified as vacancies and possibly vacancy aggregates. It appears that the method may be made sufficiently precise to serve as a tool for investigating point defects in many substances.

II. PRINCIPLES OF THE MEASUREMENTS

Lattice defect concentrations in real crystals can be investigated by a direct comparison of densities as determined by bulk and by x-ray lattice parameter measurements. For a perfect crystal $\rho = nM/vN_0$ where ρ is the bulk density, n the number of atoms/unit cell, M the atomic weight, v the unit cell volume given by x-ray measurements, and N_0 Avogadro's number. Generally, the presence of lattice imperfections will destroy equality. The most comprehensive and accurate measurements of this nature¹⁴ have indicated that data from crystals of different types can be made consistent within $1:10^5$ by using isotopic weights and relative abundances and a value of N_0 about 1.2×10^4 larger than the present accepted value. The possible defect structure remains unknown except possibly where large defect concentrations are involved. In addition, the temperature range in which direct high precision density measurements can be made is limited.

In view of the relatively imperfect character of actual crystals and of the limitations imposed by uncertainties in the absolute values of x-ray emission

⁴ Koehler, Seitz, and Bauerle, *Phys. Rev.* **107**, 1499 (1957).

⁵ Kimura, Maddin, and Kuhlmann-Wilsdorf, *Acta Met.* **7**, 145 (1959).

⁶ W. DeSorbo and D. Turnbull, *Phys. Rev.* **115**, 560 (1959).

⁷ Bacchella, Germagnoli, and Granata, *J. Appl. Phys.* **30**, 748 (1959).

⁸ A. E. Roswell and A. S. Nowick, *Trans. Am. Inst. Mining Met. Engrs.* **197**, 1259 (1953).

⁹ J. E. Bauerle and J. S. Koehler, *Phys. Rev.* **107**, 1493 (1957).

¹⁰ D. K. C. MacDonald, in *Report of the Conference on Defects in Crystalline Solids, Bristol, 1954* (The Physical Society, London, 1955), p. 383.

¹¹ L. G. Carpenter, *J. Chem. Phys.* **21**, 2244 (1953).

¹² W. DeSorbo, *Phys. Rev.* (to be published).

¹³ J. Van Duijn and J. Van Galen, *Physica* **23**, 622 (1957).

¹⁴ Smakula, Kalnajs, and Sils, *Phys. Rev.* **99**, 1747 (1955).

wavelengths and of N_0 it is clearly advantageous to use comparison methods. Such a technique is particularly useful for the study of thermally generated defects. For a cubic crystal consisting of a constant number of atoms, N , the thermal expansion can be written

$$\begin{aligned} 3(\Delta a/a) &= p(T) + r(T) + x(T), \\ 3(\Delta L/L) &= q(T) + s(T) + y(T). \end{aligned} \quad (2)$$

The reference lattice constant, a , and length, L , are taken at a temperature at which the thermally generated defect concentrations are negligible. Here $p(T)$ and $q(T)$ denote the "true" thermal expansion of the standard (admittedly imperfect) crystal without thermally generated defects, $x(T)$ and $y(T)$ denote the expansion arising directly from creation of defects, and $r(T)$ and $s(T)$ denote the thermal expansion of the crystal due to the presence of lattice defects which alters the lattice frequency distribution and therefore the internal energy.

It is expected on very general grounds that $p(T) + r(T) = q(T) + s(T)$ because, regardless of the vibration of atoms in the crystal, a time average mean position of the atoms in the unit cell is meaningful; and length and x-ray techniques measure merely changes in unit cell dimensions. At the highest temperatures, the asymmetry of the diffuse x-ray scattering¹⁵ may begin to contribute an experimental error to the measurement of the positions of Laue-Bragg interference maxima, the error depending on the particular reciprocal lattice point; for the simpler solids this error is very small.

Eshelby¹⁶ has shown that a uniform random distribution of cubically symmetric point centers of dilatation (point defects) in an elastic material with cubic elastic constants will produce a uniform elastic strain of the crystal without change of shape.† When uniform straining without change of shape occurs, the reciprocal lattice undergoes a uniform strain equal and opposite to the uniform strain of the crystal lattice; and the fractional change of lattice constant is equal to the fractional change in linear dimensions of the crystal.

For a crystal containing N atoms and ΔN identical point defects, the term $x(T)$ can be written $\Delta N f \Omega / N \Omega$ when each defect contributes a fractional expansion f of an atomic volume Ω . The term $y(T)$ is $\Delta N (f+1) \Omega / N \Omega$, if one new atomic site has appeared as a result of the creation of each defect, e.g., in vacancy production. Then

$$\Delta N / N = 3(\Delta L / L - \Delta a / a) \quad (3)$$

if the expansions are randomly directed. In the general

case where different types of defects may be present, we have

$$\Delta N / N = (c_{v1} + 2c_{v2} + 3c_{v3} + \dots) - (c_{i1} + 2c_{i2} + \dots), \quad (4)$$

where c_{v1} , c_{v2} , and c_{v3} are the fractional concentrations of monovacancies, divacancies, and trivacancies; and c_{i1} and c_{i2} are the corresponding concentrations of interstitial-type defects. We note that a measurement of $(\Delta L / L - \Delta a / a)$ yields only the net fractional increase in the number of atomic sites, $\Delta N / N$, and that it is independent not only of the lattice relaxation around the defects, f , but also of their degrees of association.

It remains to be seen how closely this model corresponds to an actual crystal. A direct experimental test of Eshelby's result has been made for copper at liquid helium temperature in which the centers of distortion were produced by deuteron irradiation.^{17,18} While the measured length and lattice parameter changes were very small, the equality $\Delta a / a = \Delta L / L$ was established within an experimental error of about 15%. Berry¹⁹ has reviewed measurements indicating that $\Delta a / a = \Delta L / L$ when solute atoms are added to form dilute solid solutions.

It is not certain whether the elastic fields of single atomic point defects in the face-centered cubic structure have cubic symmetry. For example, the vacancy and interstitial recently considered by Tewordt²⁰ possessed cubic symmetry, but his model of the interstitial crowdion did not. In the latter case the axis of the crowdion could lie along any close-packed direction of the crystal. For a crystal containing a large number of uniformly distributed crowdions which is free of external forces, one would expect the defect axes to be randomly distributed along these directions. The same considerations apply to divacancies and other of the more complicated point defects. In all of these cases the average elastic field should have cubic symmetry. This may be seen by replacing the defects by a continuous distribution of infinitesimal centers of dilatation with the same total strength and summing their effects. We conclude that Eq. (3) will still hold in such cases.

We should also expect the volume changes due to the generation or destruction of atomic sites to be isotropic. For a cubic crystal whose dimensions are large compared to the mean distance traveled by a defect during its lifetime we may expect that the defects are generated and destroyed internally at dislocation sources and sinks.²¹ The resulting average volume changes should then be isotropic for a cubic crystal containing a random distribution of dislocations. Other sites may be created or destroyed at grain boundaries or at the surface. Though the volumes of the various sites

¹⁵ See for example: H. Jahn, Proc. Roy. Soc. (London) **A179**, 320 (1942); **A180**, 476 (1942).

¹⁶ J. D. Eshelby, Acta Met. **3**, 487 (1955); *Solid State Physics*, edited by F. Seitz and D. Turnbull (Academic Press, Inc., New York, 1956), Vol. 3, p. 121.

† The writers have also shown that this result holds for the case where an appreciable fraction of the crystal may be strained beyond the elastic range (to be published).

¹⁷ R. O. Simmons and R. W. Balluffi, Phys. Rev. **109**, 1142 (1958).

¹⁸ R. Vook and C. Wert, Phys. Rev. **109**, 1529 (1958).

¹⁹ C. B. Berry, J. Appl. Phys. **24**, 658 (1953).

²⁰ L. Tewordt, Phys. Rev. **109**, 61 (1958).

²¹ J. Bardeen and C. Herring, in *Atom Movements* (American Society for Metals, Cleveland, 1951), p. 87.

differ, the mean volume for a large number will correspond exactly to the atom volume deduced from $\Omega = nM/\rho N_0$. Further aspects of the measurement of $(\Delta L/L - \Delta a/a)$ have been discussed by the writers elsewhere.²²

III. EXPERIMENTAL METHOD

An accuracy of about $1:10^5$ was desired in the measurement of both $\Delta L/L$ and $\Delta a/a$ as functions of temperature in order to obtain the difference with sufficient accuracy to detect the expected point defect concentrations. The thermal expansion contribution to $\Delta L/L$ and $\Delta a/a$ is large compared to the point defect contribution, and the problem consists of measuring a small difference between large quantities which are sensitive to small changes in temperature. Considering Eqs. (2) at slightly different temperatures T and δT and writing the thermal expansion, $\chi(T) \equiv q(T) + s(T)$, at the point $\chi(T + \delta T)$ one has

$$\Delta N/N \simeq \gamma \exp(-E_f/kT) + \delta T \{ d\chi/dT + [(1+f)E_f/kT^2] \gamma \exp(-E_f/kT) \}, \quad (5)$$

where $\gamma = g \exp(S_f/k)$ and only one predominating type of defect has been considered. For aluminum, for which γ and $|f|$ are of order unity, the error term in the curly brackets is about 3 to 4: 10^5 per degree near the melting point. Therefore if $\Delta L/L$ and $\Delta a/a$ are measured independently,² the temperature of each measurement should be known better than $\pm 0.2^\circ\text{C}$. Because it was doubtful that this accuracy could be obtained under such conditions,² an apparatus was constructed in which

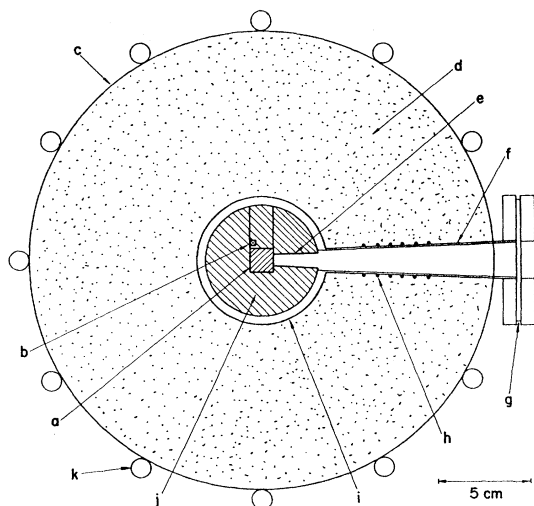


FIG. 1. Cross section of furnace at a length-measurement port. a = specimen, b = thermocouple (in quartz tube), c = outer furnace jacket, d = powdered insulation, e = viewing aperture in graphite core, f = thin-walled inconel port, g = Pyrex glass window, h = port heater winding, i = gas-tight inconel furnace tube, j = graphite core, k = water cooling tubes.

²² R. O. Simmons and R. W. Balluffi, J. Appl. Phys. 30, 1249 (1959).

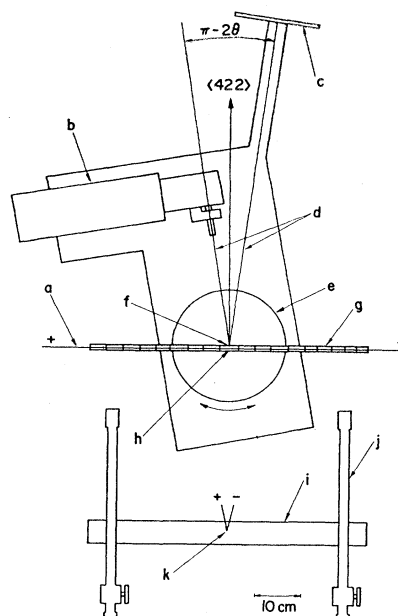


FIG. 2. Schematic top view of apparatus used for length and x-ray lattice expansion measurement. a = butt-welded Pt versus Pt-10% Rh thermocouple, b = x-ray tube and collimator, c = film cassette, d = path of incident and diffracted x-rays, e = rotating stage supporting x-ray tube platform and film cassette arm, f = vertical axis of rotation of x-ray apparatus, g = specimen (polycrystal possessing "bamboo" structure), h = x-ray crystal, i = Invar mounting bar for microscope assembly, j = filair micrometer microscope equipped with relay lens, k = thermocouple.

both $\Delta L/L$ and $\Delta a/a$ could be measured simultaneously on the same specimen and where all temperatures were measured with the same thermocouple.

1. Specimen and Furnace

The specimen, furnace arrangement, and measuring apparatus are shown in Figs. 1 and 2. A long specimen was desired in order to obtain precision in the length change measurement. The specimen, therefore, consisted of a bar, 50 cm long by 1.27 cm by 1.27 cm; it was supported in a square cross-section horizontal well machined along the axis of a large cylindrical spectrographic purity graphite core. The core provided a smooth inert support which allowed free expansion and contraction of the specimen. The graphite also protected the specimen against contamination and reduced temperature gradients by virtue of its relatively high thermal conduction.

All temperatures were measured with a butt-welded Pt versus Pt-10% Rh thermocouple²³ which was threaded through a fused quartz tube held in a second small longitudinal well in the graphite core. In this arrangement the thermocouple junction was only 3 mm

²³ The thermocouple material was obtained from S. Cohn and Company, Mt. Vernon, New York, and the temperatures reported here are believed accurate to $-0.0, +0.5$ degree C. This accuracy is of importance, of course, only in comparing the present individual measurements with the work of other investigators.

from the specimen and could be moved parallel to the specimen length in order to ascertain the temperature at any point. The high thermal conduction of the specimen and graphite insured that the actual specimen temperature was measured.

A number of special precautions were taken to produce a temperature distribution which could be maintained uniform along the entire length of the rather long specimen during the time required for each simultaneous measurement of the length and lattice parameter. A 300-cm long furnace tube and helical resistance winding were used in order to reduce the effects of thermal end losses. Also, the winding was divided into three sections for which the power input could be individually controlled. The radial thermal losses from the ports were compensated by individually controlled port heater windings. By use of these individual controls it was possible to maintain the temperature constant along the specimen length to $\pm 0.2^\circ\text{C}$ or less. The specimen temperature was kept constant in time by stabilizing the rms voltage applied to the windings, maintaining the outside jacket at constant temperature, and using the natural compensation given by the large temperature coefficient of resistance of the Pt-10% Rh windings. The furnace was, therefore, operated under steady-state conditions, and the temperature distribution never drifted in time by more than $\pm 0.2^\circ\text{C}$ during any single measurement.

The specimen was prepared from 99.995% pure aluminum bar stock²⁴ originally containing 0.003% Cu, 0.001% Fe, and 0.001% Si. The forged specimen was first machined to fit loosely into the well of the graphite core and was then annealed in the furnace for several days within several degrees of the melting point (660°C) in a prepurified nitrogen²⁵ atmosphere. Recrystallization and grain growth occurred, and a final bamboo-type grain structure was produced where single large grains, several cm in size, occupied the full width of the bar. One large grain occupying the center of the bar was found to have an orientation suitable for the x-ray diffraction measurement. This grain was chosen as the x-ray crystal and was located at the x-ray port in the final assembly. At the end of the grain growth anneal a portion of the specimen was removed; its resistance ratio between ice and liquid helium temperatures was measured and found to be 414. This value was in close agreement with the ratio for the starting material and is typical of aluminum of this purity.²⁶ These tests, therefore, indicated that purity was maintained during specimen preparation. Evidence that purity was maintained during the experiment was obtained later when it was found that

all measurements could be reproduced reversibly upon heating and cooling.

2. Length Change Measurement

The paramount considerations in the design of the present measurements of change in length were that (1) the specimen be quite free of external constraint during expansion and contraction, (2) the influence of creep²⁷ at the highest temperatures be minimized, and (3) the necessary sensitivity be obtained with very direct means, avoiding any apparatus which would be in a temperature gradient and therefore subject to possible unknown error.

$\Delta L/L$ was measured by observing the movement of reference marks on the specimen surface with two parallel mounted filar micrometer microscopes equipped with relay lenses. The microscopes, having a mechanical working distance of 13.3 cm and a magnification of 60 \times , were rigidly clamped to a massive Invar bar in order to maintain their spacing constant (Fig. 2). They were each calibrated *versus* a stage micrometer, and were thereafter operated at fixed and equal focus, the proper focusing (i.e., condition that Invar bar and specimen be parallel to one another) being achieved by rotation and translation of the whole microscope assembly. Errors due to misalignment are of the cosine type and were negligibly small in this work. The temperature of the Invar bar was measured with a thermocouple and the spacing of the telescopes was initially calibrated *versus* temperature using a quartz rod standard. Minor corrections could then be made for the temperature variation of the spacing; the final error from this source was negligible because room temperature was controlled to $\pm 1^\circ\text{C}$.

The reference marks at the ends of the specimen were made with a modified Tukon micro-hardness machine equipped with a pyramidal diamond indenter. The resulting pyramidal indentations were about 6×10^{-3} cm across the base and their apexes were used for the measurements. The detailed appearance of these marks remained constant during the experiments due to the high stability of the thin aluminum oxide film on the surface. A high precision cathetometer was used to make an initial direct measurement of the specimen length.

In a typical length measurement the temperature along the specimen length was first adjusted to a constant value ($\pm 0.2^\circ\text{C}$). At least ten consecutive pairs of microscope readings were then taken in a five to seven minute interval, and the temperature distribution along the specimen was again determined. In most cases an x-ray lattice expansion measurement was also made during this period. The final temperature assigned to the length measurement was then obtained by averaging the temperature distribution over time and distance. The temperature of the x-ray measurement

²⁴ This material was kindly donated by the Aluminum Company of America.

²⁵ Properties are listed by the supplier as purity greater than 99.996%, oxygen 0.0008%, dew point -68°C .

²⁶ A. Sosin and J. S. Koehler, Phys. Rev. **101**, 972 (1956); Chanin, Lynton, and Serin, Phys. Rev. **114**, 719 (1959).

²⁷ J. Weertman, J. Appl. Phys. **27**, 832 (1956).

was taken as the temperature at the x-ray crystal averaged over time.

3. Lattice Expansion Measurement

Characteristics required of the x-ray lattice expansion measurement included (1) high accuracy, (2) short measurement time, (3) a specimen having properties identical to those of the length change measurement specimen, and (4) careful design so that the temperature distribution would be negligibly perturbed by the necessary access port for the x-rays. The general arrangement, as shown in Fig. 2, satisfied these requirements. It is an extension of a back-reflection rotating-single-crystal technique used earlier.¹⁷

The rigid assembly, consisting of the x-ray tube with collimator and film cassette, was oscillated with a typical amplitude of 40' of arc with a period of about 2 minutes around a vertical axis intersecting the point of contact of the incident x-ray beam and the crystal surface. The oscillation was used to smooth the film exposure reproducibly. Accurate alignment of the device was obtained by careful preliminary measurements of the position of the axis of rotation. A standard full-wave rectified General Electric CA-7 x-ray tube, fitted with a 0.254-mm slit collimator of 24' angular divergence, was run at 30 kv and 13 ma. Exposure times for Ni $K\alpha_1$ radiation ($\lambda = 1.65784$ Å) diffracted by (422) planes parallel to the specimen surface were less than 7 minutes near the melting temperature (660°C), at which the Bragg angle is near 80°. A gaseous helium path was provided in order to minimize absorption of the diffracted beam. The lowest temperature at which measurements could be made was 229°C.

The position of the Laue-Bragg line on the film was measured with an average accuracy of 0.06 mm using an X cross hair on the cursor of a commercial film reader. The line width at half-maximum intensity varies with Bragg angle; near $\theta = 83^\circ$ the width was about 6 mm, the major fraction contributed by spectral width of the x-ray emission line. Film shrinkage effects due to processing were appropriately corrected using measurements on a known array of fiduciary marks placed on the film at the time of exposure.

The relation between the position of the Laue-Bragg line on the flat film and the Bragg angle, θ , was obtained in several different ways. First, the included angle ($\pi - 2\theta$) between incident and diffracted rays at a known temperature 351.5°C (at which the defect concentration is immeasurably small) was measured directly using a rigid template and the known position of the center of rotation, with an estimated accuracy of $\pm 5'$ in θ . Second, the Bragg angle at the same temperature was deduced from the accepted value of lattice parameter of aluminum²⁸ $a(20^\circ\text{C}) = 4.04911$ Å, and the measured $\Delta L/L$ between 20 and 351.5°C, the

estimated accuracy in this case being $\pm 1'$ in θ . The Bragg angles corresponding to other positions were calculated from the measured geometry of the apparatus. Third, the $\Delta a/a$ values deduced from the first and second methods were compared with the measured $\Delta L/L$ values above 229°C and the Bragg angle adjusted within the overlap of the previously mentioned error limits to produce congruence of the length and lattice parameter changes. The final adjustment produced $\Delta L/L = \Delta a/a$ over a range of 229 to 415°C with mean absolute deviations of 9×10^{-6} in $\Delta L/L$ and of 6×10^{-6} in $\Delta a/a$. Over this same temperature range $\Delta L/L = \Delta a/a$ changes by 5.31×10^{-3} . It was felt that this was a sensitive test, because the linear dispersion at the film, $\Delta a/a$ per mm, varies approximately as $\tan \theta$, which is about 15 at 229°C and only about 8 at 415°C.

There was some possibility that the local temperature at the x-ray measurement region might have been perturbed by the exposure of the specimen face at this point to the outside of the furnace. Simple calculations of radiation loss indicated that this effect was negligible. Also, the gas atmosphere within the ports was well heated by the port windings, greatly reducing temperature gradients which might have led to conduction cooling of the exposed crystal face. Possible cooling by convection was limited by the small, narrow, horizontal character of the port openings. Since no temperature perturbations were recorded by the thermocouple in the port regions when the furnace was properly adjusted, we may conclude that a uniform temperature was maintained.

Several other possible errors must be considered. Error could originate from the presence of a possible superficial film on the specimen face. The highly stable aluminum oxide film was indeed present but its thickness was small compared to the penetration of the x-rays. Further, no cumulative effects due to continued film formation during the experiment were observed; $\Delta a/a$ measurements were completely reproducible during the thermal cycling of the heating and cooling runs, which included over 125 hours above 600°C. The term "film formation" here includes a possible layer formed by penetration of impurities by diffusion. The small error due to asymmetry of the diffuse x-ray scattering,¹⁵ already mentioned in Sec. II, should be particularly small in aluminum because of the relatively high characteristic temperature (near 400°K) compared to the melting temperature (993°K). Corrections which depend upon θ due to finite specimen height and to refraction in the aluminum are negligible in the restricted range of large θ used here. The large size of the apparatus minimized the relative importance of possible errors due to inaccurate measurement of specimen-to-film distance, penetration of the x-rays into the specimen face, and eccentric placement of the vertical rotation axis, because the error distances involved all tend to have a fixed magnitude.

²⁸ W. B. Pearson, *Lattice Spacings and Structures of Metals and Alloys* (Pergamon Press, New York, 1958).

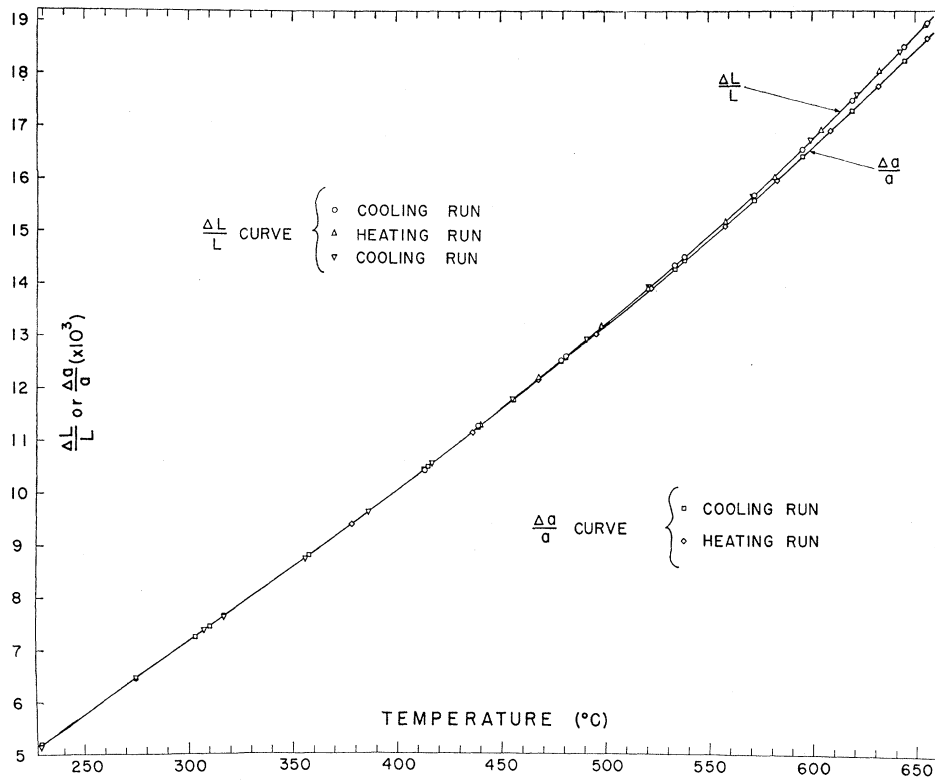


FIG. 3. Measured length and lattice parameter expansions of aluminum *versus* temperature. The fraction of additional atomic sites present in thermal equilibrium at the higher temperatures is 3 ($\Delta L/L - \Delta a/a$). These sites correspond to the thermal generation of lattice-vacancy-type defects. $\Delta L/L = \Delta a/a = 0$ at 20°C.

IV. EXPERIMENTAL RESULTS

The values of $\Delta L/L$ and $\Delta a/a$ are shown plotted in Fig. 3 for the temperature range 229–655°C with 20°C taken as the reference temperature. The $\Delta L/L$ curve includes all points taken during two heating runs and one cooling run, whereas the $\Delta a/a$ curve includes all points taken during one heating and one cooling run. The mean deviations of the experimental points from

TABLE I. Macroscopic linear thermal expansion of aluminum.

T (°C)	Present work	$10^3[\Delta L/L(20^\circ\text{C})]$						
		a	b	c	d	e	f	g
225	5.06
250	5.75
275	6.44
300	7.13	7.21	6.94	7.13	6.94	7.09 ^b	7.01	...
325	7.84
350	8.56
375	9.30
400	10.05	10.15	9.77	10.06	9.72	10.09 ⁱ	10.23	...
425	10.82
450	11.61
475	12.40
500	13.23	13.30	12.79	13.28	12.72	...	13.87	13.28
525	14.07
550	14.93
575	15.83
600	16.76	15.94	...	17.96	16.78
625	17.72
650	18.72

^a See reference 29.

^b See reference 30.

^c See reference 31.

^d See reference 32.

^e See reference 33.

^f See reference 34.

^g See reference 2.

^h Interpolated.

ⁱ Extrapolated.

the smooth $\Delta L/L$ and $\Delta a/a$ curves are 1.1×10^{-5} and 0.5×10^{-5} , respectively, and the maximum deviations are 3.5×10^{-5} and 2.0×10^{-5} , respectively. No evidence was obtained for any systematic lack of reversibility during heating and cooling. The mean deviation of all $\Delta L/L$ and $\Delta a/a$ values from the smooth curve in the temperature interval between 229°C and about 415°C is 0.8×10^{-5} . We note that the thermal expansion of aluminum, $\chi(T)$, defined earlier, cannot yet be inferred with similar accuracy at temperatures above about 415°C, because the lattice relaxations around the defects are presently unknown. Further, once these are known the "true" thermal expansion would be obtained by subtracting an amount $s(T)$, which although probably small is also presently unknown.

Values of $\Delta L/L$ and $\Delta a/a$ obtained by a number of other investigators^{2,29-37} are given in Tables I and II for purposes of comparison. All values have been converted to expansions relative to 20°C using the expansion data

²⁹ P. Hidnert, Sci. Papers Natl. Bur. Standards **19**, 697 (1923-24).

³⁰ F. L. Uffelman, Phil. Mag. **10**, 633 (1930).

³¹ C. S. Taylor *et al.*, Metals and Alloys **9**, 189 (1938).

³² H. Esser and H. Eusterbrock, Arch. Eisenhüttenw. **14**, 341 (1941).

³³ F. C. Nix and D. MacNair, Phys. Rev. **60**, 597 (1941).

³⁴ J. W. Richards, Trans. Am. Soc. Metals **30**, 326 (1942).

³⁵ Esser, Eilender, and Bungardt, Arch. Eisenhüttenw. **12**, 157 (1938).

³⁶ A. J. C. Wilson, Proc. Phys. Soc. (London) **54**, 487 (1942).

³⁷ E. C. Ellwood and J. M. Silcock, J. Inst. Metals **74**, 457, 721 (1948).

of Nix and MacNair³³ near room temperature. The present $\Delta L/L$ measurements fall in between the previous values, and are in good agreement with those of Taylor *et al.*³¹ and those of Feder and Nowick² up to 600°C. However, the present data show a considerably larger increase between 600°C and the melting point than was observed by Feder and Nowick. The $\Delta a/a$ data are all in quite good agreement near 300°C. However, near 600°C the present values are somewhat lower than the others but are still in fair agreement with those of Feder and Nowick.²

At about 420°C $\Delta L/L$ becomes noticeably greater than $\Delta a/a$ and this difference continuously increases up to the melting point. The reversible nature of the high-temperature divergence of the two curves confirms the isotropic and reversible behavior of the defect source and sink action. The net fractional change of the number of atomic sites, $\Delta N/N$, was calculated from the smooth curves using Eq. (3) and is plotted logarithmically versus $1/T$ in Fig. 4. The estimated maximum absolute measuring error in $\Delta N/N$ is about $\pm 4 \cdot 10^5$, and this uncertainty is indicated for each point. We note that the possible percentage error is relatively small at the highest temperatures (about $\pm 5\%$) but becomes considerably larger at the lower temperatures ($\pm 40\%$). The data follow the expected Arrhenius type behavior, and the equation for the indicated line through the data points is $\Delta N/N = \exp(2.4) \exp(-0.76 \text{ ev}/kT)$.

V. INTERPRETATION AND DISCUSSION

Net fractional changes in the number of atomic sites, $\Delta N/N$, during heating and cooling have been determined experimentally, and it remains to interpret these results in terms of the presence of point defects. The fact that $\Delta N/N$ is positive establishes vacancy-type

TABLE II. Lattice parameter thermal expansion of aluminum.

T (°C)	Present work	$10^3[\Delta a/a(20^\circ\text{C})]$			
		a	b	c	d
225	5.06
250	5.75
275	6.44
300	7.13	7.4 ± 0.4^e	7.15
325	7.84	7.80^f	...
350	8.56
375	9.30
400	10.05	10.7 ± 0.4^e	10.13	10.08^f	...
425	10.81
450	11.59
475	12.37
500	13.18	14.1 ± 0.4^e	...	13.29^f	...
525	14.01
550	14.85
575	15.71
600	16.60	17.6 ± 0.4^e	16.74	16.80^f	16.68
625	17.51
650	18.44	...	18.60

^a See reference 35.

^b See reference 36.

^c See reference 37.

^d See reference 2.

^e Values picked off smooth curve.

^f Interpolated.

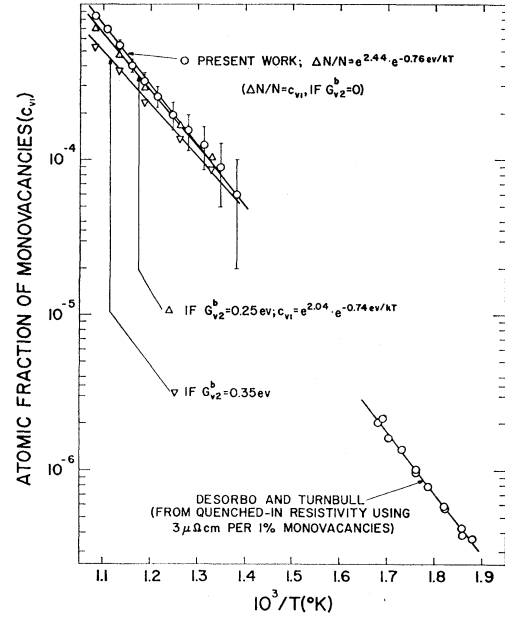


FIG. 4. Monovacancy concentration, c_{v1} , versus $1/T$ (°K) for aluminum. Values are shown for three different assumed divacancy binding energies, G_{v2} .

defects as the dominant defects (see Eq. 4), in agreement with much previous expectation¹ based upon the large calculated energies of formation of interstitial defects in copper.³⁸ Further, measurements of the electrical resistivity of aluminum at high temperatures³⁹ can be interpreted satisfactorily by considering as predominant only defects having essentially the same formation energy as obtained in the present work. We assume, therefore, that the concentrations of the interstitial-type defects are small enough to be ignored.

We are left to a consideration of the concentrations of the various vacancy-type defects which may be present. Each type of defect will exist in an independent equilibrium in the crystal at concentrations given by

$$\begin{aligned} c_{v1} &= \exp(-G_{v1}^f/kT), \\ c_{v2} &= 6 \exp(-G_{v2}^f/kT), \\ c_{v3} &= 8 \exp(-G_{v3}^f/kT), \end{aligned} \quad (6)$$

where the G_j^f are the free energies of formation, exclusive of configurational entropy, and where we assume that a divacancy consists of a pair of nearest neighbor vacancies and that a trivacancy consists of a triangular group of nearest neighbor vacancies. Other less close-packed clusters consisting of two or three vacancies may be visualized. However, their formation energy should increase as the degree of close-packing decreases and their concentrations should, therefore, be relatively small.

³⁸ H. B. Huntington, Phys. Rev. **91**, 1092 (1953).

³⁹ R. O. Simmons and R. W. Balluffi, following paper [Phys. Rev. **117**, 62 (1960)].

TABLE III. Fraction of atomic sites associated with monovacancies, divacancies, and trivacancies for different possible binding energies.

T (°C)	G_{v2}^b (ev)	G_{v3}^b (ev)	$c_{v1} \times 10^4$	$2c_{v2} \times 10^4$	$3c_{v3} \times 10^4$
480	0.15	0.30	1.07	0.01	0.00
	0.25	0.50	1.02	0.06	0.00
	0.35	0.70	0.87	0.20	0.01
520	0.15	0.30	1.74	0.03	0.00
	0.25	0.50	1.64	0.13	0.00
	0.35	0.70	1.37	0.38	0.02
570	0.15	0.30	3.12	0.09	0.00
	0.25	0.50	2.89	0.31	0.01
	0.35	0.70	2.35	0.82	0.05
610	0.15	0.30	5.25	0.24	0.00
	0.25	0.50	4.75	0.72	0.02
	0.35	0.70	3.72	1.65	0.12
650	0.15	0.30	7.91	0.48	0.01
	0.25	0.50	7.00	1.36	0.04
	0.35	0.70	5.35	2.80	0.25

The concentrations of the defects depend upon the binding energies, $G_{v2}^b = 2G_{v1}^f - G_{v2}^f$ and $G_{v3}^b = 3G_{v1}^f - G_{v3}^f$. By combining Eqs. (4) and (6) we obtain

$$24 \exp(G_{v3}^b/kT)c_{v1}^3 + 12 \exp(G_{v2}^b/kT)c_{v1}^2 + c_{v1} = \Delta N/N, \\ c_{v2} = 6c_{v1}^2 \exp(G_{v2}^b/kT), \quad (7) \\ c_{v3} = 8c_{v1}^3 \exp(G_{v3}^b/kT).$$

The defect population may be completely determined from the experimental data by use of Eqs. (7) if G_{v2}^b and G_{v3}^b are known. It will be shown below that higher order clusters may almost certainly be safely neglected. Unfortunately, there are no completely reliable values of G_{v2}^b and G_{v3}^b presently available. Most estimates of G_{v2}^b in face-centered cubic metals fall in the range $0.1 < G_{v2}^b \leq 0.4$ ev.^{1,4-6} Brooks⁴⁰ points out that the energy of a vacancy cluster is crudely proportional to its "surface area"; if the vacancies are taken as cubes, it follows that $G_{v3}^b \simeq 2G_{v2}^b$.

With this approximation, we have used Eqs. (7) to calculate the expected concentrations of the different defects for a range of possible binding energies, viz., $G_{v2}^b = 0.15, 0.25$, and 0.35 ev. The results are given in Table III in terms of the fraction of atomic sites which is associated with monovacancies, divacancies, and trivacancies. The clusters become relatively more abundant as either the binding energy or the temperature increases. The concentrations of sites associated with trivacancies are seen to be negligible for present purposes under all conditions, since they never exceed about half the estimated maximum measuring error of $\Delta N/N$. The concentrations of divacancies are more difficult to evaluate, and are seen to be appreciable at higher temperatures if G_{v2}^b exceeds about 0.15 ev. DeSorbo and Turnbull⁶ have carried out annealing experiments in quenched aluminum and interpret certain features of their work to mean that $G_{v2}^b \simeq 0.3$ ev $-(E_{v1}^m - E_{v2}^m)$, where E_{v1}^m and E_{v2}^m are the energies

of motion of monovacancies and divacancies.⁴¹ If $(E_{v1}^m - E_{v2}^m) \simeq 0.15$ ev,⁴ then G_{v2}^b is in the range 0.15 ev. It must be emphasized, however, that these results are highly tentative. While it appears probable that G_{v2}^b is closer to the value 0.15 than to the value 0.35 ev, this result is by no means proven.

It should be pointed out in this connection that the majority of the relative divacancy concentrations in Table III are probably consistent with typical self-diffusion data for face-centered cubic metals. No evidence has yet been found in these metals of any divacancy contribution to high-temperature self-diffusion.⁴² Unfortunately, self-diffusion has not yet been measured in aluminum. Nevertheless, it is worthwhile to estimate crudely the self-diffusion contributions which would be expected from the monovacancy and divacancy concentrations in Table III, and to show that they are probably consistent with usual diffusion data for other face-centered cubic metals. The self-diffusion coefficient due to monovacancies may be written as⁴³

$$D_1 \simeq \nu_1 a^2 \exp(S_{v1}^m/k) \exp(-E_{v1}^m/kT) c_{v1},$$

where we assume only atom-vacancy exchange between nearest neighbors and where correlation has been neglected. S_{v1}^m is the entropy of motion and ν_1 is a frequency. The corresponding diffusion coefficient due to divacancies is

$$D_2 \simeq (\frac{1}{3}) \nu_2 a^2 \exp(S_{v2}^m/k) \exp(-E_{v2}^m/kT) 2c_{v2},$$

where we assume that the only atoms which jump into a divacancy have both divacancy sites as nearest neighbors and where correlation is again neglected. Since the nearest neighbor relaxation is greater around a divacancy than a monovacancy, and since there is less lattice straining when an atom jumps into a divacancy than a monovacancy, we take $\nu_1 = 2\nu_2$ and $S_{v1}^m = 2S_{v2}^m = 2k$. If $(E_{v1}^m - E_{v2}^m)$ is again taken to be 0.15 , the ratio of diffusivities is $D_1/D_2 \simeq 2.5(c_{v1}/2c_{v2})$ at 660°C . This result, combined with the defect concentrations given in Table III, indicates that the divacancy diffusion component would be difficult to detect, in agreement with usual self-diffusion data.

In view of the possibility that G_{v2}^b may exceed 0.15 ev, and that divacancies may be present in appreciable concentrations, Fig. 4 shows the expected monovacancy concentrations for different assumed binding energies. On the assumption that $G_{v2}^b \leq 0.25$ ev, S_{v1}^f lies in the range 2.0 to 2.4 entropy units, and E_{v1}^f lies in the range 0.74 to 0.76 ev.⁴⁴ These values are quite consistent with the generally expected values of these quantities. The

⁴¹ Unknown entropy factors have been neglected in these estimates.

⁴² C. E. Birchenall, Met. Revs. 3, 235 (1958).

⁴³ A. D. LeClaire, Acta Met. 1, 438 (1953).

⁴⁴ No attempt will be made here to carry along estimates of the uncertainty of each value of the energy or entropy quoted, since, in general, these uncertainties cannot be established with any precision. For example, estimates of the uncertainty based upon the scatter of data points are usually unrealistic.

⁴⁰ H. Brooks, in *Impurities and Imperfections* (American Society for Metals, Cleveland, 1955), p. 1.

positive sign of S_{v1}^f agrees with the usual prediction⁴⁵ that there is a loosening of the lattice in the vicinity of the vacancy and a corresponding decrease in the vibrational frequencies. The magnitude of S_{v1}^f suggests that vacancies in aluminum are relatively simple and are not disordered regions involving a comparatively large number of atoms.^{46,47} The present formation energy may be combined with the energy of motion of monovacancies in order to estimate the activation energy for self-diffusion, Q . From kinetic studies of very high purity material quenched from comparatively low temperatures,⁶ $E_{v1}^m = 0.65$ ev and, therefore, $E_{v1}^m + E_{v1}^f = 1.40$ ev $= Q$. This value agrees with the value $Q = 1.4 \pm 0.1$ ev found by Spokas and Slichter⁴⁸ using nuclear magnetic resonance techniques and with the value $Q = 1.43 \pm 0.08$ ev estimated by Nowick⁴⁹ from an analysis of alloy diffusion data.

It is of considerable interest to compare the present equilibrium vacancy measurements with the defect concentrations which have been retained in aluminum by quenching. The latest, and probably most reliable, quenching data⁵⁰ have been used for this purpose, and monovacancy concentrations derived from these data are also shown in Fig. 4. According to the present results, the imperfections present in thermal equilibrium in this lower temperature interval between about 260 and 320°C were almost certainly monovacancies. The quenched-in resistivity increments were converted to monovacancy concentrations using a value for the monovacancy resistivity of $3 \mu\text{ohm-cm/atomic } \%$.³⁹ Extrapolations of the curves giving the best fit through the present high-temperature equilibrium data and the best curve through the lower temperature quenching data indicate that the derived quenched concentrations are somewhat low compared to the high-temperature concentrations. However, the disagreement is no larger than a factor of about two.

It is also apparent that an over-all curve may be

TABLE IV. Values for the entropy of formation, S_{v1}^f , and energy of formation, E_{v1}^f , of monovacancies according to different methods.

Method	S_{v1}^f/k	E_{v1}^f (ev)
Used present high-temperature equilibrium data only, assuming $G_{v2}^b = 0$.	2.4	0.76
Used present high-temperature equilibrium data only, assuming $G_{v2}^b = 0.25$ ev.	2.0	0.74
Used lower temperature quenching data only, with $\Delta\rho = 3 \mu\text{ohm-cm/at. } \%$ vacancies.	2.4	0.79
Used best fit through both high-temperature equilibrium data and low-temperature quenching data assuming $G_{v2}^b = 0.15$ ev.	3.6	0.86
Used high-temperature resistance data ^a only.	...	0.77

^a See reference 39.

drawn through both the high- and low-temperature data without appreciably violating the probable ranges of uncertainty of the data. Values of S_{v1}^f and E_{v1}^f have been calculated from the curve giving the best fit through both the equilibrium data points and the quenching data points on the assumption that $G_{v1}^b = 0.15$ ev. The results are given in Table IV along with a summary of the values obtained by all the other methods. As expected, the values obtained by forcing a fit through the high- and low-temperature data are somewhat larger than the values obtained by the other methods. We note, however, that the larger values obtained from the over-all fit are not inconsistent with the known properties of aluminum, and therefore must be considered as possible values.

The result that the high- and low-temperature data show an apparent disagreement which may be as large as a factor of two may be due to several reasons. Among these are: (1) lattice anharmonicity effects may partially invalidate the methods used to derive the value of $3 \mu\text{ohm-cm/atomic } \%$ of monovacancies. In this case the resistivity increment per vacancy would be smaller than estimated, and the quenched-in concentration would be correspondingly greater; (2) the high-temperature divacancy concentrations may be greater than expected leading to smaller monovacancy concentrations (i.e., G_{v2}^b may be > 0.25 ev); (3) all of the equilibrium defects may not have been retained in the quenching experiments. Further discussion of these possibilities is given in the following paper.³⁹

⁴⁵ C. Zener, J. Appl. Phys. **22**, 372 (1951).

⁴⁶ See discussion of this point by W. M. Lomer in: *Vacancies and Other Point Defects in Metals and Alloys* (The Institute of Metals, London, 1958), p. 79.

⁴⁷ Huntington, Shirn, and Wajda, Phys. Rev. **99**, 1085 (1955).

⁴⁸ J. J. Spokas and C. P. Slichter, Phys. Rev. **113**, 1462 (1959).

⁴⁹ A. S. Nowick, J. Appl. Phys. **22**, 1182 (1951).

⁵⁰ W. DeSorbo and D. Turnbull, Acta Met. **7**, 83 (1959).